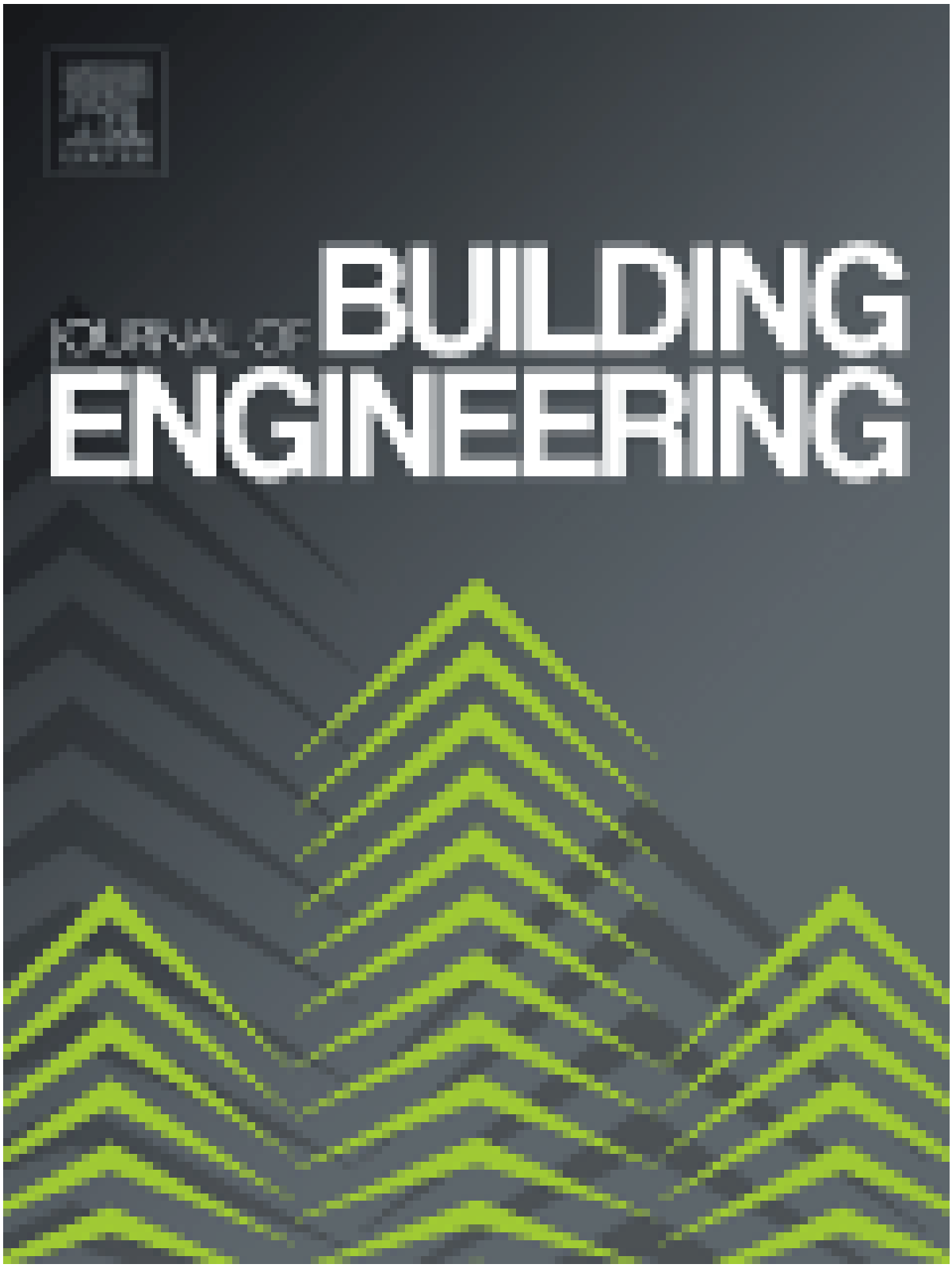
JOURNAL OF
BUILDING
ENGINEERING

Tensile Behaviour of Textile Reinforcement under Accelerated Ageing Conditions

Natalie Williams Portal, Ph.D.[1], Mathias Flansbjer, Adj. Prof.[2], Pär Johannesson, Ph.D.[3], Katarina Malaga, Adj. Prof.[4], Karin Lundgren, Prof.[5]

[1]CBI Swedish Cement and Concrete Research Institute, Borås, SE-501 15, Sweden, and Dept. of Civil and Environmental Engineering, Chalmers University of Technology, Gothenburg 412 96, Sweden E-mail: Natalie.WilliamsPortal@cbi.se

[2]SP Technical Research Institute of Sweden, Borås, SE-501 15, Sweden, and Dept. of Civil and Environmental Engineering, Chalmers University of Technology, Gothenburg 412 96, Sweden E-mail: Mathias.flansbjer@sp.se

[3]SP Technical Research Institute of Sweden, Gothenburg, SE-400 22, Sweden, E-mail: Par.Johannesson@sp.se

[4]CBI Swedish Cement and Concrete Research Institute, Borås, SE-501 15, Sweden, E-mail: Katarina.Malaga@cbi.se

[5]Dept. of Civil and Environmental Engineering, Chalmers University of Technology, Gothenburg 412 96, Sweden, E-mail: Karin.lundgren@chalmers.se

Abstract:

Textile Reinforced Concrete (TRC) has emerged as a promising alternative wherein corrosion is no longer an issue and much thinner and light-weight elements can be designed. Although TRC has been expansively researched, the formalization of experimental methods concerning durability arises when attempting to implement and design such innovative building materials. In this study, accelerated ageing tests paired with tensile tests were performed. The change in physico-mechanical properties of various commercially available textile reinforcements was documented and evaluated. The ability for the reinforcements to retain their tensile capacity was also quantified in the form of empirical degradation curves. It was observed that accelerated test parameters typically applied to fibre-reinforced polymer (FRP) bars and grids are generally too aggressive for the textile reinforcement products and alternative boundary conditions are necessary. The developed degradation curves were found to have an overall good correlation with the experimental findings.

Keywords: Textile reinforced concrete; accelerated ageing; tensile testing; experimental tests; durability.

1. Introduction

Textile reinforced concrete (TRC) not only presents sustainable advantages [1] but has also been found to be a suitable material for structures such as thin cladding and sandwich elements [2, 3]. These alternative reinforcement materials are typically made of alkali-resistant (AR) glass, basalt or carbon fibres and offer a much lower density (1800-3000 kg/m^3) in comparison to steel reinforcement bars (7850 kg/m^3) which further contributes to a reduction in dead weight. Nonetheless, questions regarding the long-term durability arise when attempting to design and implement new building materials such as TRC, as there is minimal long-term performance or durability data available [4, 5].

TRC can be generally characterized as a three-phase material consisting of a cementitious matrix, fibre-yarn structure as well as a fibre-matrix interface. This heterogeneous material can be exposed to various degradation processes over its service life, such as fibre degradation due to chemical attack, fibre-matrix interfacial physical and chemical interactions, and volume instability and cracking [6]. These degradation processes can occur individually or simultaneously which in turn makes the characterization of the long-term performance of fibre-based composites complex. Another aspect which is critical to understand is that fibre-based reinforcement materials are marked by small surface defects or weak zones resulting from production and handling processes [7]. These defects have been found to be one of the factors contributing to strength loss of the final reinforcement product. Particularly concerning glass fibres, these weak zones have been observed to consequently grow when exposed to sustained loading conditions as a result of a mechanism called static fatigue or delayed failure [7, 8]. The static fatigue strength of the composite is related to the critical flaw size, stress level and exposure conditions which govern the crack growth rate of surface defects [9].

Individual fibres incorporated in the yarns which form the textile reinforcement grid are typically composed of a sizing material applied during production which serves primarily as a

surface protection [10]. This applied sizing could greatly influence the degradation process and long-term performance of the composite [11-13], particularly concerning AR-glass and basalt fibres. During the service life, TRC and the reinforcement could face such boundary conditions like the high alkalinity of the concrete pore water (peak during hydration), varying temperature and humidity loads, carbonation as well as sustained and cyclic loading and fatigue which could all have an effect on its long-term mechanical behaviour. As such, the critical zones of degradation will most likely be the fibre sizing-coating and the fibre-matrix interface.

Durability performance is most accurately measured in real-time [5]; however, typically having time as a constraint, accelerated ageing tests [6] or experimentally calibrated models [10] have been used to predict the long-term performance of textile reinforcement, fibres or fibre-reinforced polymers (FRP) in a cementitious matrix. A common method to accelerate the ageing of fibres in the form of FRP rods or textile reinforcement consists of immersing them in a simulated or actual concrete pore solution, i.e. alkaline environment, while simultaneous being exposed to high temperature [10, 14]. For instance, this method has been used to measure the loss of tensile strength exclusively due to the so-called chemical corrosion process related to AR-glass textile reinforcement [15]. Alternatively, basalt or glass fibre yarns have been immersed in sodium hydroxide (NaOH) and hydrochloric acid (HCl) solutions for varying time periods [16] or 3-ionic solutions to target localized attack [17, 18]. Electron-microscopes have commonly been applied to investigate the degradation phases of the fibre-yarn surface [18] or the fibre-yarn-matrix interface [13]. Accelerated ageing of textile reinforcement cast in concrete has also been conducted in climate chambers at varying temperatures or moisture conditions followed by the quantification of loss of tensile strength and bond through various mechanical tests [4, 13, 19, 20]. A time-dependent model was even developed and calibrated to determine the strength loss of AR-glass textile reinforcement in TRC [21-23], which was thereafter applied to design a pedestrian bridge [24]. Although a number of accelerated tests have been reported in this field of study,

researchers have applied varying experimental methods and have investigated differing materials making them subjective and to some degree non-comparable.

2. Research significance

In this study, accelerated tests paired with direct tensile tests were performed according to ISO 10406-1 [25] pertaining to fibre-reinforced polymer (FRP) bars and grids. It was of key interest to forecast the so-called long-term mechanical behaviour and material degradation of various commercially available textile reinforcement products for potential use in new façade solutions. Alternative boundary conditions were also included in the scope of work to investigate the discrete influence of two key variables on material ageing, i.e. temperature and pH of a simulated pore solution. The change in physico-mechanical properties of the various textile reinforcements was documented and evaluated in this work. The ability for the reinforcement materials to retain their tensile capacity was also quantified in the form of empirical degradation curves. The study also included development of methods for preparation of end anchorage, gripping system to the testing machine and measurement of strain up to failure.

3. Experimental program

3.1 Textile reinforcement

AR-glass, basalt and carbon textile reinforcement grids primarily selected based on the current availability of commercial products were investigated. TRC building applications have primarily focused on the use of AR-glass and carbon fibre materials, but natural and polymer fibres have also been researched for this application [5]. The use and durability of AR-glass has been deeply investigated for use in TRC as it has been both cost effective and readily available [21]. Alternatively, basalt fibres, mineral fibres extracted from volcanic rock, are often compared to glass fibres, such as E-glass and AR-glass, due to existing similarities in their chemical composition [11, 16, 26]. Regarding carbon fibre materials, the price per square meter of product is still significantly higher than the other alternatives, which is

primarily because it is still most commonly demanded in other industries such as automotive and aerospace. General material and mechanical properties are commonly provided by the textile reinforcement producers, such as those data presented in Table 1, and at times also including the modulus of elasticity and elongation. The methods used to obtain the mechanical properties vary based on the source, which could decrease the soundness of the available data. Even so, tensile testing of these reinforcement materials was conducted according to the standard method stated in ISO 10406-1 [25] to base further evaluations in this study on these obtained data.

Table 1: General properties of the studied reinforcement materials.

Material (Product/Supplier)	Coating	Grid Spacing 0°/90° [mm]	Weight [g/m^2]	Tensile Strength of Yarn [N]
AR-glass (Glasfiberväv Grov), Sto Scandinavia AB	Styrene-butadiene resin (SBR), 20 %	7/8	210	>400
Basalt (Mesh-10-100), Sudaglass Fiber Technology Inc.	Undisclosed resin, 17 %	10/10	165	1152
Carbon (SIGRATEX Grid 250-24), SGL Group	Styrene-butadiene resin (SBR), 15 %	17/18	250	4243

3.2 Test specimen preparation

The mechanical properties and durability of the selected textile reinforcement materials were investigated. Specimen preparation and test methods provisioned in ISO 10406-1 [25] were applied to determine the tensile capacity, tensile rigidity and ultimate strain of the textile reinforcement alternatives pre- and post-immersion into an alkaline solution. The textile reinforcement, initially in the form of a grid, was cut into so-called individual yarns with a remaining 2 mm projection of the cross-points (crossbars) as well as more than three cross-points along the length.

The method applied for gripping the specimens in tensile tests is known to be crucial for the test results, and various methods have previously been evaluated for tensile tests of FRP-bars [27]. The method must be suitable for the given specimen geometry while transmitting

only the tensile force along the longitudinal axis of the specimens. It should also be ensured that premature failure of the specimen does not take place in the grip zone which is an undesirable failure mode. Accordingly, various types of end anchorage were evaluated in this study which led to the conclusion that an aluminium tube with epoxy resin was the most suitable method as it allows for the tensile force to be transmitted to the specimen by shear stress within the epoxy. Other gripping methods, such as clamp-to-yarn, emery cloth, rubber sheets and aluminium tabs were found to underestimate the tensile strength of the material which resulted in the specimens to either slide out of the test grip or fail within the grip.

The aluminium tubes used as end anchorage had a length ranging from 75-100 mm, outer diameter of 15 mm and inner diameter of 12 mm. The inside of the tubes were roughened and cleaned with acetone to achieve superior bonding with the epoxy. An epoxy resin with 10 % sand filler (NM Injection 300, Nils Malmgren AB) was used. A special device was developed to keep the specimens and the tubes concentrically and vertically aligned during the epoxy setting, such that 14 specimens could be prepared simultaneously. The specimen ends were prepared in two phases; one end was firstly cast in the aluminium tube followed by a 24 h hardening period of the epoxy, thereafter the specimen was upturned and the second end was prepared using the same procedure. The total specimen length was 500 mm and the end anchorage length, L_e, was 75 – 100 mm on either side of the specimen as depicted in Figure 1. The tested length, L, was set to 300 – 350 mm which meets the minimum specified length of ≥ 300 mm. In addition, the gauge length of the extensometer measuring the strain, L_g, was 100 mm.

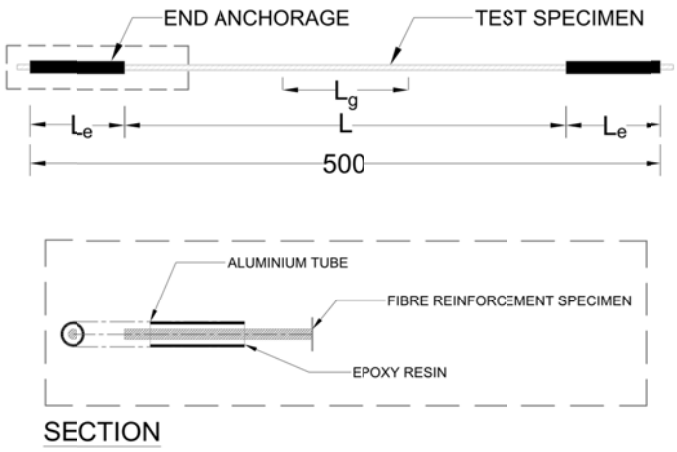

Figure 1. Geometry and layout of a tensile test specimen with end anchorage.

3.3 Tensile strength test

Tensile strength tests were conducted in accordance with ISO 10406-1. The tests were carried out using a universal testing machine (Sintech Model 20/D) and the force was recorded by a load cell with a rated capacity of 10 kN and an accuracy better than 1 %. The deformation was measured by a Messphysik Videoextensometer ME46 with backlight technique as illustrated in Figure 2. The measuring gauge length was chosen as approximately 100 mm as previously mentioned and was marked by two reference metal cross-pins. A great advantage of using a video extensometer is that it is possible to measure the deformation up to failure of the specimen, i.e. the ultimate strain can be determined directly. A mechanical extensometer most often has to be removed before failure to avoid risk of damage, thereby causing the ultimate strain to be extrapolated by the assumption of linear elasticity. The force and deformation were recorded in a data acquisition system with a sampling rate of 20 Hz. The load was introduced to the specimen by gripping the end anchorages in the conventional hydraulic grips of the testing machine. A clamp pressure of 4 MPa was applied to the anchorage at both ends. The specimens were generally preloaded by a force of 20 N; however, in certain cases a larger preload of approximately 100 N was needed to adequately straighten out the specimens in order to obtain correct deformation measurements. The tests were controlled by the cross-head displacement of 3 mm/min,

corresponding to a strain rate of approximately 5 x 10^{-3}/min within the measuring length. The average temperature during testing was measured to be 25°C. Tensile tests of at least five test samples of each reinforcement material were conducted for pre- and post- immersion conditions.

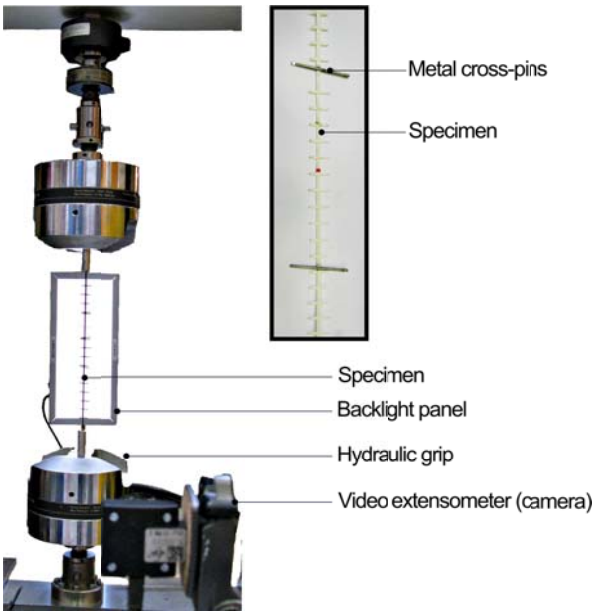

Figure 2. Overview of the tensile test setup and reference metal cross-pins.

3.4 Alkali resistance test

The alkali resistance of the reinforcements was also investigated according to ISO 10406-1 [25]. The test consists of immersing linear pieces of textile reinforcing grid with extraneous parts cut away in an alkaline solution (pH>13) while being exposed to a temperature of 60 ±3°C for 30 days. The prepared alkaline solution should have a similar pH value to that of the pore solution of concrete in order to simulate the environment in which textile reinforcement could face when embedded in a concrete matrix. The alkaline solution provided in the standard consists of 8.0 g of sodium hydroxide (NaOH) and 22.4 g of potassium hydroxide (KOH) in 1 l of deionized water. The alkalinity of this solution was measured to be approximately pH 14.

The linear test pieces were bundled and sealed by epoxy resin end caps to prevent infiltration of the solution. The linear test pieces were thereafter immersed in the alkaline

solution in plastic cylindrical containers illustrated in Figure 3. The plastic containers were sealed and placed in a climate chamber. Test specimens were immersed during 5, 10, 20 and 30 days to enable the quantification of the gradual degradation of the material. Once removed from the alkaline solution, the test specimens were rinsed in dionized water and visually examined prior to commencing with the end anchorage preparation for tensile testing. The test specimens were not subjected to any tensioning load during the period of immersion.

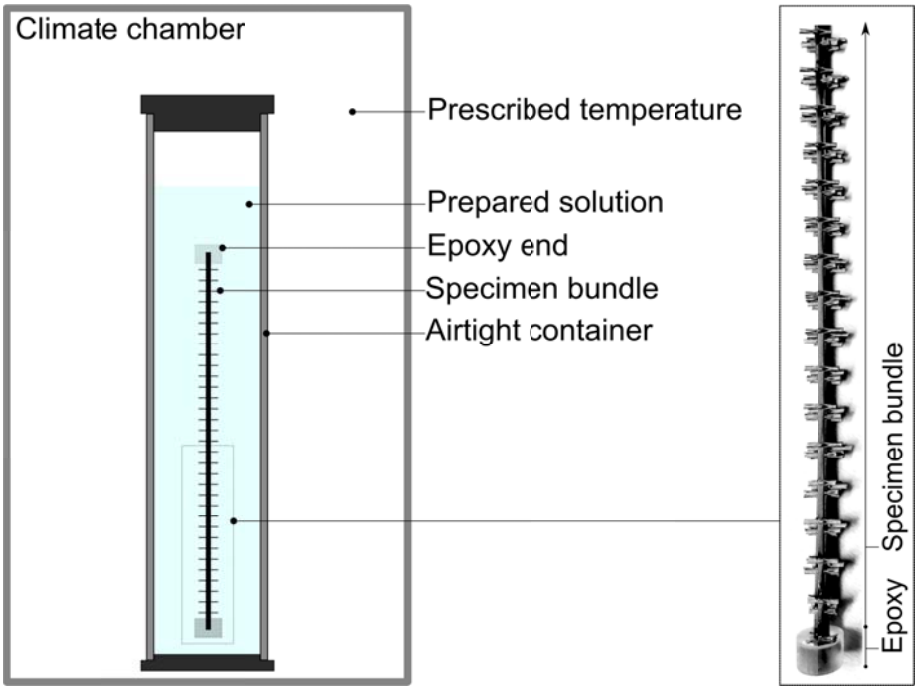

Figure 3. Specimen bundle exposed to the test boundary conditions.

One main drawback of this standard test method is such that it does not lead to the quantification of the actual lifespan of the reinforcement materials, yet it allows for a relative comparison of how the materials withstand the prescribed boundary conditions. Secondly, the boundary conditions are thought to overestimate the realistic conditions encountered by reinforcement embedded in a concrete matrix [10]. Thirdly, these suggested conditions may not be suitable for all the tested materials because they have differing physical and chemical processes leading to degradation [6]. Therefore, samples were also immersed in deionized water (pH 7) and exposed to a temperature of 60 ±3°C for 30 days to observe the sensitivity

of the fibres to temperature. Then again, test samples immersed in both pH 7 and pH 14 were exposed to room temperature (20 ±3°C) for 10 days to determine whether the high alkaline solution could be the controlling degradation parameter. An experimental test matrix, shown in Figure 4, depicts the various cases included, as well as how these tests were carried out during the course of the study. The presented test IDs, i.e. C0, B0 and A0, will be referred to throughout the remaining text.

Case	Effect	Temperature [°C]	pH Value [-]	Time [days]	Carbon	Basalt	AR-glass
Reference	No exposure	20	-	0	C0	B0	A0
1	High temperature + high pH (ISO 10406-1)	60	14	5	C1-5	B1-5	A1-5
				10	C1-10	B1-10	A1-10
				20	C1-20	B1-20	A1-20
				30	C1-30	B1-30	A1-30
2	High temperature + neutral pH	60	7	30	C2	B2	A2
3	Low temperature + high pH	20	14	10	C3	B3	A3
4	Low temperature + neutral pH	20	7	10	C4	B4	A4

Performed ageing only
Performed ageing + tensile test
Not tested

Figure 4. Overview of the experimental test matrix.

4. Results

4.1 Visual observations

The visual observations noted after the alkali resistance tests are reported in this section. The external appearance of the textile reinforcement specimens was examined pre- and post-immersion, for comparison of colour, surface condition and change in shape.

The carbon textile reinforcement pre-immersion specimen (C0) was compared to the associated post-immersion specimens (C1-10, C1-20, C1-30, C2). After 10-30 days of immersion in pH 7 and pH 14 at 60°C, there was no significant visible change of colour or surface texture and all samples were intact. According to these results, accelerated testing using the alternative boundary conditions, so-to-say Cases 3 and 4, was not conducted.

The basalt textile reinforcement post-immersion specimens (B1-5, B1-10, B1-20, B1-30, B2, B3, and B4) were compared to the reference pre-immersion specimens (B0). The B1-5 specimens were not marked by any major visual changes and could be tested in tension. This product however showed signs of degradation after 10 days of immersion in the standard conditions, which included colour change and the start of coating separation towards the surface. The remaining specimens exposed to the standard conditions (B1-20, B1-30) were also marked by colour change and what appears to be the lifting of the coating to the surface, which is exemplified in Figure 5. These post-immersed specimens lost a great deal of physical strength to the point that they either broke during the handling process (B1-10) or prior to removal from the solution (B1-20, B1-30) and therefore could not undergo tensile testing. It should be noted that the cross-points were a particular weak point in the structure, such that the coating built up in these locations and caused the cross-threads to lift and the samples to break at these localized points.

In order to obtain a better understanding of the cause of such extensive deterioration, specimens were also immersed in a solution of pH 7 at 60 ±3°C for 30 days (Case 2). The observed degradation was similar to the specimens exposed to the standard conditions, yet these could be further tested in tension. Moreover, to verify if the elevated temperature of

60°C was the governing factor in this equation, specimens were also immersed in pH 7 and pH 14 for 10 days at 20 ±3°C (Cases 3 and 4). The samples exposed to both of these alkalinity levels, namely B3 and B4, had a slight build-up of coating at the cross-points and minor colour change. The B3 samples had a loss of strength to the extent that they could be broken with a slight pulling force at the cross-points.

Figure 5. Visual comparison between pre- (B0) and post-immersion (B1-30) for the basalt product.

The visual observations for the AR-glass textile reinforcement exposed to all conditions were compared to the pre-immersion samples (A0). The reinforcement pieces exposed to the standard conditions (A1-5, A1-10, A1-20, A1-30) were marked by the loss of the majority of cross-threads which revealed a thinner layer of sizing in these locations, wherein an example is shown in Figure 6. These samples also lost a significant amount of physical strength and could be easily broken by hand at the cross-points. Similar observations to those described for the samples which faced the standard conditions were also noted for Case 2 (A2). Specimens exposed to Case 3 (A3) had a slightly wavy structure, yet had retained sufficient physical strength. Lastly, those immersed according to Case 4 (A4) were intact with most cross-threads and could not be easily torn apart.

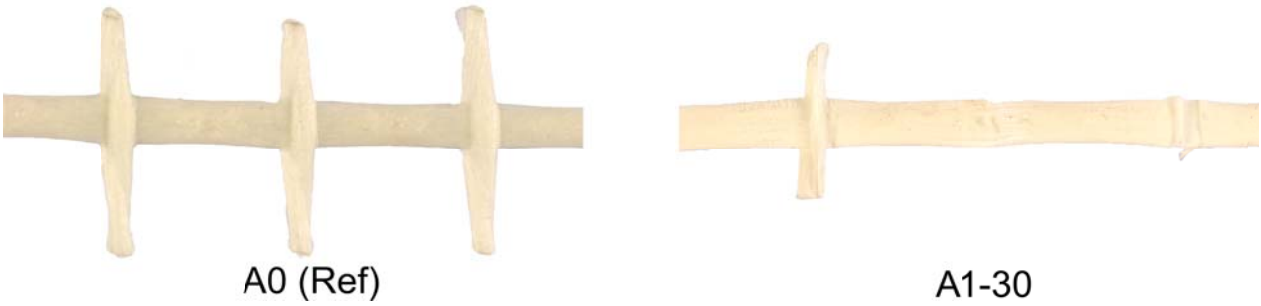

Figure 6. Visual comparison between pre- (A0) and post-immersion (A1-30) for the AR-glass product.

4.2 Tensile tests

Tensile tests were performed on the selected textile reinforcement materials for pre- and post-immersion conditions. In the case where tensile tests could not be conducted due to the extent of sample degradation, particularly concerning basalt and AR-glass, additional tensile tests related to alternative boundary conditions were thus conducted. The primary mechanical properties extracted from the tensile test results consisted of the ultimate tensile capacity, F_u, and ultimate strain ε_u. The tensile rigidity, E_A, was calculated from the load-strain relation as the secant modulus between the load level at 20 % and 50 % of the tensile capacity. Furthermore, the tensile capacity retention rate, R_{ET}, and tensile rigidity retention rate, R_{EA}, which can be used to measure the relative mechanical degradation of the post-immersed reinforcement specimens were computed. The tensile capacity retention rate is defined as per ISO 10406-1 [25] and the tensile rigidity retention rate is included in this work as an additional comparative parameter. The retention rates are described as per Equations 1 and 2:

$$R_{ET} = (F_{u1}/F_{u0}) \cdot 100 \quad (1)$$

$$R_{EA} = (E_{A1}/E_{A0}) \cdot 100 \quad (2)$$

where, F_{u0} is the tensile capacity and E_{A0} is the tensile rigidity pre-immersion, and F_{u1} is the tensile capacity and E_{A1} is the tensile rigidity post-immersion, all values in Newton.

A compilation of the mean tensile test results along with the associated standard deviations are reported in Table 2. Furthermore, the tensile test results for the pre-immersed (reference) samples are compared to the post-immersed ones in terms of applied load versus strain in Figure 7. It should be noted that the strain is shifted from zero by an indicated change in strain for various data sets to enhance the overall visual clarity.

Table 2: Mean tensile test results (standard deviation in parentheses).

Case		Reinforcement type	Tensile capacity, F_u (σ) [kN]	Ultimate strain, ε_u (σ) [%]	Tensile rigidity, E_A (σ) [kN]	Tensile capacity retention rate, R_{ET} (σ) [%]	Tensile rigidity retention rate, R_{EA} (σ) [%]
Reference	Pre-immersion	Carbon (C0)	1.88 (0.23)	0.87 (0.06)	221.38 (5.05)	-	-
		Basalt (B0)	0.62 (0.03)	2.85 (0.08)	23.73 (0.49)	-	-
		AR-glass (A0)	0.41 (0.02)	1.91 (0.10)	22.49 (0.49)	-	-
1	60°C, pH 14, 30 d (ISO 10406-1)	Carbon (C1-30)	2.36 (0.03)	1.01 (0.03)	235.68 (18.60)	125 (2)	106 (8)
		Basalt (B1-5)	0.02 (0.01)	-	-	3 (2)	-
		Basalt (B1-10, B1-20, B1-30)	Not measurable				
		AR-glass (A1-5)	0.14 (0.03)	-	-	33 (7)	-
		AR-glass (A1-10, A1-20, A1-30)	Not measurable				
2	60°C, pH 7, 30 d	Carbon (C2)	2.14 (0.21)	0.91 (0.14)	234.33 (6.75)	114 (11)	106 (3)
		Basalt (B2)	0.39 (0.01)	1.70 (0.10)	23.13 (0.66)	62 (2)	97 (3)
		AR-glass (A2)	0.15 (0.03)	0.73 (0.10)	20.54 (2.62)	35 (7)	91 (12)
3	20°C, pH 14, 10 d	Basalt (B3)	0.32 (0.02)	1.37 (0.08)	23.38 (0.98)	52 (3)	99 (4)
		AR-glass (A3)	0.27 (0.01)	1.37 (0.11)	19.75 (1.43)	65 (3)	88 (6)
4	20°C, pH 7, 10 d	Basalt (B4)	0.56 (0.05)	2.52 (0.23)	24.11 (0.58)	90 (8)	102 (2)
		AR-glass (A4)	0.40 (0.04)	1.77 (0.17)	23.15 (0.59)	97 (10)	103 (3)

The tensile behaviour of all the reinforcements depicted in Figure 7 have a brittle material behaviour signifying that there is no intermediate yielding point, and as such failure occurs upon reaching the ultimate stress. Concerning the carbon textile reinforcement, there is a general increasing trend noted for all measured and calculated parameters. The basalt and AR-glass samples aged according to the standard conditions of Case 1 were not measurable due to the extent of degradation with the exception of specimens aged for five days (B1-5, A1-5); wherein the strain up to failure could not be measured due to the fragility of the aged specimens. When exposed to Cases 2 and 3, the tensile capacity and the ultimate strain were observed to significantly decrease. Based on Figure 7, no particular remarks could be made regarding the effect of Case 4.

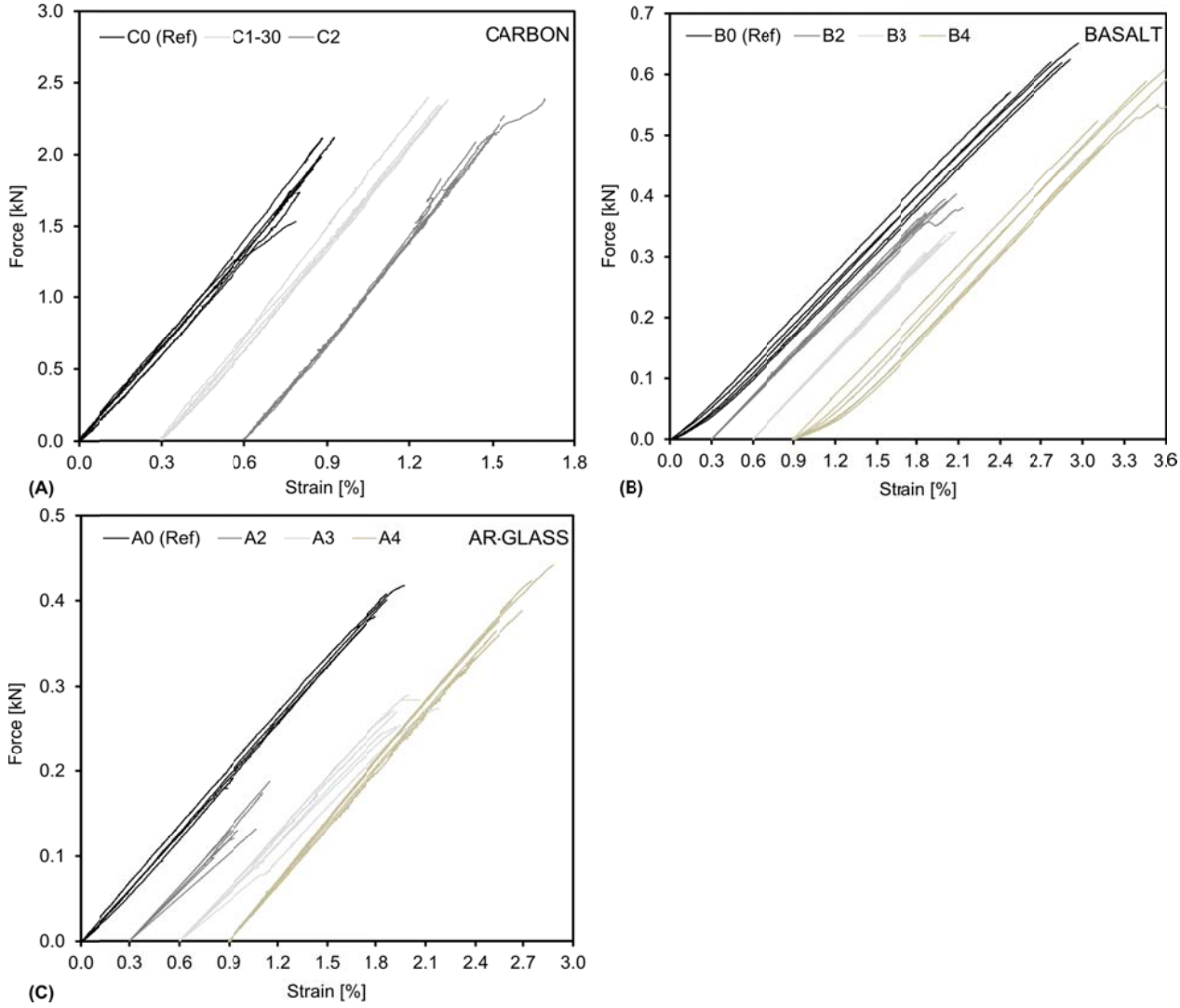

Figure 7. Applied load versus strain of tested textile reinforcement samples: a) Carbon, b) Basalt and c) AR-glass (note the differing scales).

5. Discussion

5.1 Retention rates

The tensile capacity and rigidity retention rates are graphically illustrated for the sake of comparing the mean values, data scatter and confidence intervals for all tested cases. The tensile capacity and rigidity retention rates shown in Figure 8 were statistically evaluated using a two-sample t-test procedure assuming equal variances and corresponding to a confidence interval of 95 %. Respective 95 % confidence intervals were thereafter calculated based on these statistical data according to common statistical methods for two samples found in e.g. Montgomery, Runger, et al. [28]. The calculated confidence interval is shown to indicate whether or not the mean value is significantly different from the reference. From this type of comparison, existing trends in the retention rates can be depicted and confirmed for each reinforcement alternative.

The carbon textile reinforcement samples exposed to the standard conditions of 60°C, pH 14, 30 days (Case 1) appear to have a significant increase in tensile capacity and no change in tensile rigidity. The results pertaining to the samples aged for 60°C, pH 7, 30 days (Case 2) indicate no major change in tensile capacity but a notable increase in tensile rigidity. The cause of the noted increase is likely related to the stiffening of the applied resin at high temperatures which has also been observed in Hegger, Horstmann, et al. [3]. Moreover, these results correlate with the notion that carbon fibres in the form of FRP and textile reinforcement are thought to be chemically inert as they have been found to be resistant to alkaline-induced deterioration [14, 29] and possess a general high resistance to chemical environments [5].

To further analyse the retention rates pertaining to AR-glass, it is necessary to describe possible degradation mechanisms typically affecting glass fibres which are categorized accordingly: 1) chemical attack of filaments by alkalies (corrosion) [30] , 2) static fatigue or delayed failure of filaments resulting from surface flaws [7, 8], and 3) mechanical attack due

to matrix densification [19]. Similar degradation mechanisms have also been reported for basalt fibres, yet it should be noted that basalt fibres possess differing chemical compositions whereby a high iron content may be responsible for an inferior alkali-resistance [11, 31].

It can be further ascertained from Figure 8, that a discernible loss of tensile capacity of AR-glass has taken place for all cases except for 20°C, pH 7, 10 days (Case 4). A clear decrease in tensile rigidity was observed for AR-glass for 20°C, pH 14, 10 days (Case 3). Moreover, the lowest tensile capacity retention rates were noted as 33 % and 35 % under the conditions of 60°C, pH 14, 5 days (Case 1) and 60°C, pH 7, 30 days (Case 2), respectively. It has been stipulated by others that the deterioration of AR-glass textile reinforcement increases with increasing pH value and also with temperature [5, 19], which also correlates with the reported findings. In other studies, AR-glass fibres exposed to high temperatures (50-60°C) while placed in a cement environment, i.e. pore solution, were found to face significant strength loss [8, 30]. It was also reported in Chen, Davalos, et al. [32] that glass fibre reinforced polymer bars had most significant strength loss for solutions at 60°C. As aforementioned, the underlying deterioration mechanism related to glass are fairly complex, yet it can be pressumed here that the observed strength loss is attributed to a combination of chemical attack and static fatigue of the reinforcement.

A noticeable decay in tensile capacity for the basalt textile reinforcement samples were marked for Cases 1 (60°C, pH 14, 5 days), 2 (60°C, pH 7, 30 days) and 3 (20°C, pH 14, 10 days). This product had the lowest tensile capacity retention rate of 3 % (Case 1) followed by 52 % (Case 3) which may indicate its sensitivity to high alkalinity. As for the samples exposed to 20°C, pH 7, 10 days (Case 4), the upper bound of the confidence interval for the tensile capacity borders the reference baseline such that this decrease in capacity is uncertain. Also, the resulting loss in tensile rigidity can be concluded as insignificant in comparison to the reference mean value. On the whole, basalt fibres have been described as having a low alkaline resistance despite the accelerated ageing conditions and exposure medium, i.e. pore solution or concrete matrix. Depending on the exposure medium, however,

differing degradation mechanism have been noted, such as the formation of thick corrosion surface layers or pitting formation [11]. Despite the use of additional surface coatings commonly applied to AR-glass, e.g. styrene-butadiene, basalt fibres still show extensive loss of mechanical performance due to the dissolution of the surface leading to loss of cross-sectional area [12].

Furthermore, it is interesting to note the slight difference between the tensile capacity retention of AR-glass (65 %) and basalt (52 %) under exposure Case 3. From these results, it can be stipulated that both materials are being dissolved by chemical attack by alkalis since these are fundamentally made of silicon dioxide (SiO_2), thereby leading to structure and strength loss [7, 16, 33]. As previously mentioned, certain basalt products have been found to have a lower resistance to an alkaline environment compared to AR-glass products. Based on these findings, however, it could solely be deduced that the particular applied styrene-butadiene sizing could potentially be providing additional surface protection in the case of AR-glass.

As previously mentioned, the retention rates for both basalt and AR-glass were nearly unmeasurable for the standard conditions with the exception of those specimens tested after 5 days of ageing (Case 1). Alternatively, in such cases, the measurement of the residual yarn or fibre diameter as demonstrated in Förster and Mäder [10] could be applied in further studies to yield complementary results and to observe the influence of the applied sizing [11]. The analysis of the chemical degradation of the material, i.e. in terms of surface morphology, could also be worth examining, similar to a study by Wei, Cao, et al. [16], in order to more accurately target the source of degradation.

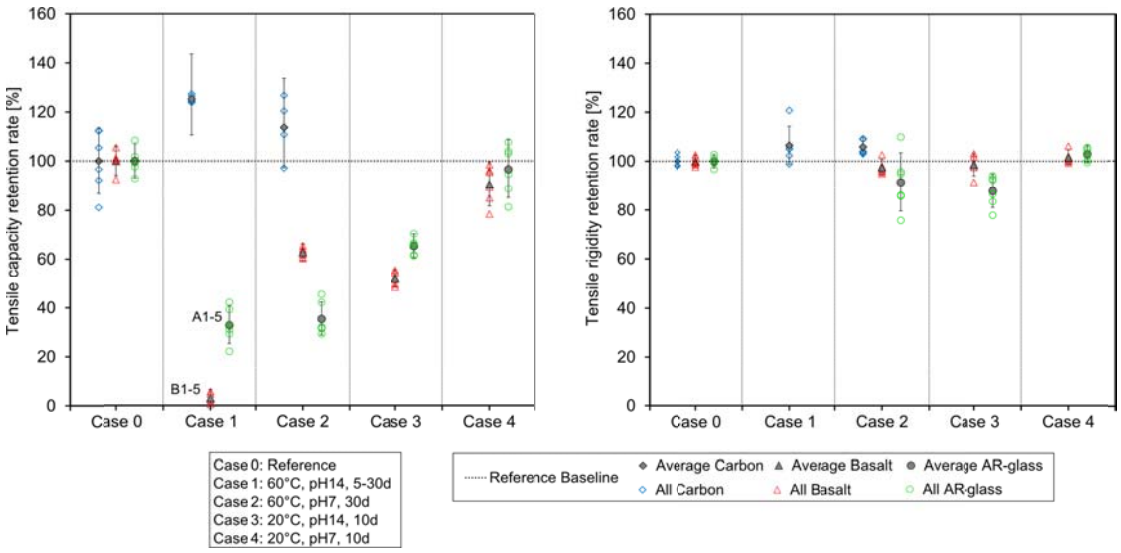

Figure 8. The tensile capacity retention rate (left) and tensile rigidity retention rate (right).

5.2 Variable sensitivity

Multiple-linear regression has been applied to correlate certain of the independent variables, which are included in the accelerated testing, namely temperature and time. The regression was applied separately to specimens aged at pH 7 and pH 14, due to the large difference between these values associated to logarithmic scale. It should be noted that the chemical constitution of the textile reinforcement products and chemical composition of the ageing solution are also independent variables which have an important impact on the degradation but are explicitly excluded from this scope for the sake of obtaining an empirical model based on the outputs of the standard ISO 10406-1 [25] test method. Based on the experimental test matrix (see Figure 4) and presented test data (see Table 2), it was concluded that multi-variable regression is solely possible for AR-glass and basalt as carbon was only tested when the temperature and time variables were simultaneously at three upper bound values. As an initial trial, the degradation of the tensile capacity, denoted as *y*, related to AR-glass and basalt reinforcement products is assumed to follow an exponential model, also applied in Cuypers, Orlowsky, et al. [23] where the logarithmic of the tensile capacity is taken as per Equations 3 and 4:

$$\ln(y) = a + b_1 \cdot t + b_2 \cdot (T-20) \cdot t = a + b \cdot (T) \cdot t \quad (3)$$

$$y=\exp(a + b\cdot(T)\cdot t) = \exp(a)\cdot\exp(b\cdot(T)\cdot t) \quad (4)$$

where, t is time in days; T is temperature in °C; a is the intercept representing the reference tensile capacity at 20°C and 0 days; the regression coefficients b_1, and b_2 represent the degradation per time unit: b_1 for the reference (20°C, 0 days), and b_2 for the effect of increased temperature. Thus, the degradation per time unit can be formulated as a function of temperature, viz. $b\cdot(T)= b_1 + b_2\cdot(T-20)$. In Equation 4, the first term, exp(a), is equivalent to the mean tensile capacity in kN, while the second term, $\exp(b\cdot(T)\cdot t)$, is the tensile capacity retention rate in percent. The three parameters can be estimated using multiple-regression which are summarized in Table 3 and plotted in Figure 9 along with the relevant experimental results. The degradation curves presented for the tested basalt and AR-glass products are empirically based on the plotted experimental results. These curves depict an initial trial to correlate and present the data obtained from the ISO 10406-1 [25] test method. A good agreement was found between the degradation curves and the experimental data. However, it is important to state that there exists underlying uncertainty in these curves which could be further improved by means of additional experiments at varying boundary conditions. Since no results could be measured from 10 to 30 days at pH 14 and 60°C, this part of the degradation curve cannot be validated for either basalt or AR-glass. There is also a scatter in the associated data at 5 days giving rise to uncertainty. Furthermore, these presented curves are based on the fact that the entire degradation of the product will follow an exponential model, which may not be the case if a given turning point was to occur in the degradation behaviour. Other sources of error could be related to the continued degradation reaction of the specimens due to entrapped test solution taking place after removal from the accelerated testing environment until conducting the experiment.

Table 3: Table with regression coefficients (standard deviation in parentheses).

Products	pH value	Regression coefficients [-]			Reference mean tensile capacity [kN]
		Intercept, a	b_1	b_2	
Basalt	7	-4.83E-01 (2.77E-02)	-1.03E-02 (3.75E-03)	-1.33E-04 (8.10E-05)	0.62 (0.03)
	14	-4.83E-01 (2.60E-01)	-6.54E-02 (3.52E-02)	-1.74E-02 (1.57E-03)	
AR-glass	7	-8.92E-01 (5.80E-02)	-3.88E-03 (7.85E-03)	-7.77E-04 (1.70E-04)	0.41 (0.02)
	14	-8.92E-01 (6.40E-02)	-4.29E-02 (8.67E-03)	-4.57E-03 (3.64E-04)	

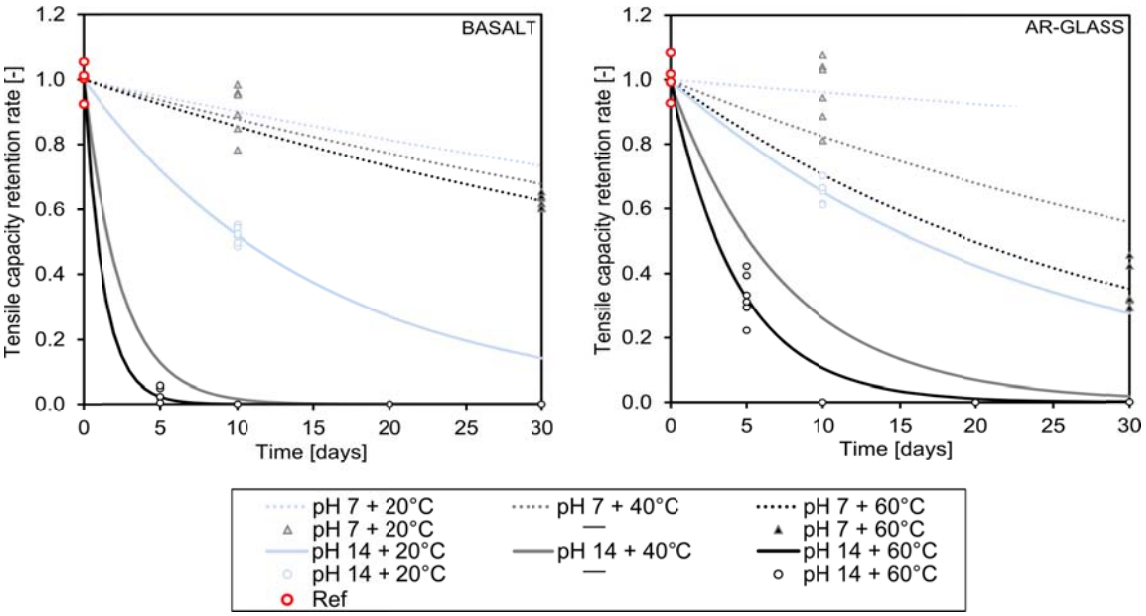

Figure 9. Empirical degradation curves for the selected basalt and AR-glass products.

This illustrated method could be further validated by means of additional data sets. Since the boundary condition specified by the standard ISO 10406-1 [25] test was too aggressive, particularly for the basalt and AR-glass textile reinforcement grids, it is suggested that the accelerated testing technique could be altered. For instance, textile reinforcement samples could be subjected to various tensioning loads during accelerated ageing, whereby time upon failure becomes an independent variable. As well, testing could also be conducted in an actual concrete pore solution or better yet in a concrete matrix instead of a pure alkaline solution. In reality, the reinforcement will not be in direct contact with alkalis when cast in concrete as the movement of alkali are said to be partly restricted by the solid porous

material [10]. Alternatively, given a façade panel application, the reinforcement will likely not be found in a constant state of wetness during service life such that wetting and drying cycles could be a more appropriate testing method [6]. The findings obtained from this experimental study could be used to predict the strength retention as a function of real time while reflecting the actual environmental conditions of the intended use according to a similar approach proposed by Dejke [10]. A larger data set corresponding to the same test solution, e.g. pH 14, is however required to enable a correlation in terms of a time shift factor, TSF (see [10]).

6. Conclusions

The tensile behaviour of selected textile reinforcement products was investigated under accelerated ageing conditions as per ISO 10406-1 [25]. It was observed that the tested carbon textile reinforcement has a superior alkali and temperature resistance, while the standard conditions were found to be too aggressive for the tested basalt and AR-glass products causing them to have nearly unmeasurable capacity after ageing. Testing the reinforcement grids according to alternative accelerated ageing schemes yielded significant trends, whereby the AR-glass product was found to be temperature sensitive particularly at 60°C and could retain more tensile strength (65%) than basalt (52%) while being exposed to 20°C, pH 14, 10 days. It is thought that the type and amount of applied sizing has a significant impact on these observed results. Empirical exponential models of the degradation of the tensile retention rate were developed as a function of temperature and time for the basalt and AR-glass products; the models were calibrated through linear regression. The models had an overall good correlation with the experimental data, yet could be further verified by means of additional experiments. Furthermore, the carbon reinforcement grid's tensile capacity and rigidity were generally maintained under all tested conditions, thus signifying favourable durability properties. Despite it having the highest initial cost, it is thought that its enhanced durability could provide a long-term payback. It is important to note that the conclusions reached in this study cannot be directly applied to

other textile reinforcement materials or fibres as each material differs in terms of chemical composition, fabrication and applied sizing. The main drawback of this applied test method is the fact that the simulated pore solution may have overestimated or inadequately represented realistic boundary conditions of textile reinforcement in a concrete matrix.

This work also included the development of methods which could be used to support those pertaining to tensile tests in the ISO 10406-1 [25] standard such as the preparation and selection of end anchorage, as well as a method to measure the strain up to failure. In further studies, it could be worth investigating a larger experimental sample size, alternative temperature and time ranges, wetting/drying cycles, test solutions and degradation of materials subject to tensioning load during ageing. It could also be valuable to analyse the chemical degradation processes affecting the surface structure of the reinforcement. Overall, there remains a need for an accelerated ageing test method tailored to TRC, as well as a database or model that can predict the residual tensile strength (and/or long term performance) of various textile reinforcement products according to real-time degradation due to varying mechanical and environmental load conditions.

Acknowledgments

The presented research was made possible with the support of the European Community's Seventh Framework Programme under grant agreement 608893 (H-House) and FORMAS IQS (Tekocrete II – Energy efficient thin façade elements for retrofitting of Million Programme housing: TRC textile reinforced concrete façade elements). More information about the H-house research project can be found at www.h-house-project.eu.com.

References

[1] Mobasher B. Mechanics of fiber and textile reinforced cement composites: CRC press; 2012.

[2] Shams A, Horstmann M, Hegger J. Experimental investigations on Textile-Reinforced Concrete (TRC) sandwich sections. Composite Structures. 2014;118:643-53.

[3] Hegger J, Horstmann M, Feldmann M, Pyschny D, Raupach M, Büttner T, et al. Sandwich Panels Made of TRC and Discrete and Continuous Connectors. In: Brameshuber W, editor. International RILEM Conference on Material Science - 2nd ICTRC - Textile Reinforced Concrete - Theme 1. Aachen RILEM Publications SARL; 2010. p. 381-92.

[4] Mumenya S, Tait R, Alexander M. Mechanical behaviour of Textile Concrete under accelerated ageing conditions. Cement and Concrete Composites. 2010;32(8):580-8.

[5] Mechtcherine V. Towards a durability framework for structural elements and structures made of or strengthened with high-performance fibre-reinforced composites. Construction and Building Materials. 2012;31:94-104.

[6] Bentur A, Mindess S. Fibre reinforced cementitious composites: CRC Press; 2006.

[7] Purnell P, Short NR, Page CL. A static fatigue model for the durability of glass fibre reinforced cement. Journal of Materials Science. 2001;36(22):5385-90.

[8] Orlowsky J, Raupach M, Cuypers H, Wastiels J. Durability modelling of glass fibre reinforcement in cementitious environment. Mater Struct. 2005;38(2):155-62.

[9] Ortlepp S, Jesse F. Experimental investigation of static fatigue strength of textile reinforced concrete. 1st International RILEM Conference on Textile Reinforced Concrete (ICTRC): RILEM Publications SARL; 2006. p. 131-40.

[10] Dejke V. Durability of FRP reinforcement in concrete: literature review and experiments. Gothenburg: Chalmers University of Technology; 2001.

[11] Scheffler C, Förster T, Mäder E, Heinrich G, Hempel S, Mechtcherine V. Aging of alkali-resistant glass and basalt fibers in alkaline solutions: Evaluation of the failure stress by Weibull distribution function. Journal of Non-Crystalline Solids. 2009;355(52):2588-95.

[12] Hempel S, Butler M, Mechtcherine V. Bond Behaviour and Durability of Basalt Fibres in Cementitious Matrices. In: Brameshuber W, editor. 3rd ICTR International Conference on Textile Reinforced Concrete Aachen, Germany: RILEM SARL; 2015. p. 225-33.

[13] Butler M, Mechtcherine V, Hempel S. Experimental investigations on the durability of fibre–matrix interfaces in textile-reinforced concrete. Cement and Concrete Composites. 2009;31(4):221-31.

[14] Micelli F, Nanni A. Durability of FRP rods for concrete structures. Construction and Building Materials. 2004;18(7):491-503.

[15] Cuypers H, Orlowsky J, Raupach M, Büttner T. Durability aspects of AR-glass-reinforcement in textile reinforced concrete, Part 1: Material behaviour. In: Grosse CU, editor. Advances in Construction Materials 2007: Springer Berlin Heidelberg; 2007. p. 381-8.

[16] Wei B, Cao H, Song S. Tensile behavior contrast of basalt and glass fibers after chemical treatment. Materials & Design. 2010;31(9):4244-50.

[17] Förster T, Plonka R, Scheffler C, Mäder E. Challenges for Fibre and Interphase Design of Basalt Fibre Reinforced Concrete. International RILEM Conference on Material Science: RILEM Publications SARL; 2010. p. 57-66.

[18] Förster T, Mäder E. Performance of Modified Basalt Fibres. Proceedings of the 18th International Conference on Composite Materials (ICCM18), Korean Society for Composite Materials2011.

[19] Butler M, Mechtcherine V, Hempel S. Durability of textile reinforced concrete made with AR glass fibre: effect of the matrix composition. Mater Struct. 2010;43(10):1351-68.

[20] Scheffler C, Gao S, Plonka R, Mäder E, Hempel S, Butler M, et al. Interphase modification of alkali-resistant glass fibres and carbon fibres for textile reinforced concrete II: Water adsorption and composite interphases. Composites Science and Technology. 2009;69(7):905-12.

[21] Büttner T, Orlowsky J, Raupach M, Hojczyk M, Weichold O, Brameshuber W. Enhancement of the Durability of Alkali-resistant Glass-Rovings in concrete. International RILEM Conference on Material Science. Germany: RILEM Publications SARL; 2010. p. 333-42.

[22] Orlowsky J, Raupach M. Durability model for AR-glass fibres in textile reinforced concrete. Mater Struct. 2008;41(7):1225-33.

[23] Cuypers H, Orlowsky J, Raupach M, Büttner T, Wastiels J. Durability aspects of AR-glass-reinforcement in textile reinforced concrete, Part 2: Modelling and exposure to outdoor weathering. In: Grosse CU, editor. Advances in Construction Materials 2007: Springer Berlin Heidelberg; 2007. p. 389-95.

[24] Hegger J, Kulas C, Schneider H, Brameshuber W, Hinzen M, Raupach M, et al. TRC Pedestrian Bridge-Design, Load-bearing Behavior and Production Processes of a Slender and Light-weight Construction. In: Brameshuber W, editor. International RILEM Conference on Material Science - 2nd ICTRC - Textile Reinforced Concrete - Theme 1. Aachen: RILEM Publications SARL; 2010. p. 353-64.

[25] ISO 10406-1. Fibre-reinforced polymer (FRP) reinforcement of concrete - Test Methods. Part 1: FRP bars and grids. Switzerland: International Organization for Standardization; 2008.

[26] Van de Velde K, Kiekens P, Van Langenhove L. Basalt fibres as reinforcement for composites. Proceedings of 10th international conference on composites/nano engineering, University of New Orleans, New Orleans, LA, USA2003. p. 20-6.

[27] Castro PF, Carino NJ. Tensile and nondestructive testing of FRP bars. Journal of composites for construction. 1998;2(1):17-27.

[28] Montgomery DC, Runger GC, Hubele NF. Engineering statistics. 5th ed: John Wiley & Sons; 2011.

[29] Scheffler C, Gao S, Plonka R, Mäder E, Hempel S, Butler M, et al. Interphase modification of alkali-resistant glass fibres and carbon fibres for textile reinforced concrete I: Fibre properties and durability. Composites Science and Technology. 2009;69(3):531-8.

[30] Majumdar AJ, West JM, Larner L. Properties of glass fibres in cement environment. Journal of Materials Science. 1977;12(5):927-36.

[31] Scheffler C, Förster T, Mäder E. Beschleunigte Alterung von Glasfasern in alkalischen Lösungen: Einflüsse auf die mechanischen Eigenschaften (Accelerated aging of glass fibers in alkali solutions: Influence on the mechanical properties). In: Curbach M, Jesse F, editors. 4th Colloquium on Textile Reinforced Structures (CTRS4). Dresden, Germany2009. p. 63-74.

[32] Chen Y, Davalos JF, Ray I, Kim H-Y. Accelerated aging tests for evaluations of durability performance of FRP reinforcing bars for concrete structures. Composite Structures. 2007;78(1):101-11.

[33] Militký J, Zeisbergerová J, Kovačič V. Chemical degradation of basalt fibers. http://centrum.tul.cz/centrum/centrum/3Aplikace/3.2_publikace/[3.2.13].pdf: Technical University of Liberec; 2009.